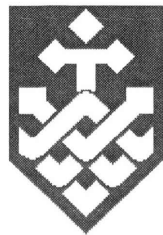


PHOTOCATALYSIS HYBRID SYSTEM IN REMOVING ORGANIC MATTER FROM WATER

By
Nathaporn Areerachakul



**Submitted in fulfillment for the degree of
Doctor of Philosophy**

**Faculty of Engineering
University of Technology, Sydney (UTS)**

Australia

2007

Certificate

I certify that this thesis has not already been submitted for any degree and is not being submitted as part of candidature for any other degree.

I also certify that the thesis has been written by me that any help that I have received in preparation of the thesis, and all sources used, has been acknowledged in this thesis.

Signature of Candidate

Production Note:
Signature removed prior to publication.

.....

Abstract

Conventional processes used to treat water and wastewater mainly removes the suspended solids, pathogens and biodegradable organic matter. The majority of persistent organic pollutants are not generally removed by these processes.

Persistent organic pollutants (POPs) constitute a class of anthropogenic substances (man-made) and can be found as trace quantity elsewhere in environment. They are toxic and bio-accumulate in humans, plants, animals, and have significant adverse impacts on human health and the environment, even at very low concentrations. They may cause cancer and disorders in the reproductive and immune systems as well as affecting the human developmental process. POPs do not readily break down in the environment with half-lives in soils in the order of years, although they may be transformed both physically and chemically over long periods of time. They exist in agricultural runoff, drainage to the sewerage system and industrial discharge.

In this study, three organic pollutants were selected for investigation humic acid as natural organic matter (NOM), metsulfuron methyl herbicide as POP, and biological treated sewage effluent (BTSE).

In the first part of the study, removal of humic substance representing NOM was investigated with various types of photocatalytic reactors. The percentage of dissolved organic carbon (DOC) removal with a batch reactor with titanium dioxide (TiO_2) as the photocatalyst ranged from 20 to 60 %. When powdered activated carbon (PAC) was added together with TiO_2 in the photo reactor, an improvement of more than twice DOC removal was noticed compared with the same amount of TiO_2 used alone. From these

results, the use of PAC - TiO₂ demonstrated superior removal of humic substance within a shorter contact time and higher removal efficiencies compared with using TiO₂ alone. Solid phase micro extraction coupled with Gas Chromatography and Flame ionisation detector (SPME/GC FID) equipped with DB-5 column was used to investigate the intermediate photo products during the photo-catalytic reaction. The manner in which intermediate photoproducts evolve and transform was demonstrated by the GC FID peak. The photo reaction can be summarised in the following way. The photo resistant by-products was adsorbed on the PAC-TiO₂ surface as shown in GC peak results. From DOC measurements, it is estimated that less than 25 % of the initial material remained. It is noted that during the PAC-TiO₂ batch process humic substance was removed immediately without forming a large amount of intermediate macromolecules of humic substance.

In the photocatalysis continuous reactor, the humic substance removal efficiency was studied at different detention time (different flowrates). Better results were achieved at longer detention times as there was more contact time. When the PAC was added, the results also indicate that the photo-catalytic adsorption hybrid system removed a significant amount of humic substance (80% DOC removal) within a shorter contact time compared with using TiO₂ alone.

In a recirculated continuous plug flow reactors the factors for controlling removal rates in heterogeneous catalysis are mass transfer and surface reaction controls. These factors were improved when a high recirculation flow rate of 250 mL/min was used where flow is turbulent. When a small amount of PAC was added in addition to TiO₂, DOC removal improved to 80% in a shorter operation time of less than 10 minutes. The results with

various types of reactors indicate that recirculated continuous reactor gave the highest efficiency for removal of NOM (humic substance) in a shorter detention time.

In the second part of the study, the removal efficiency of metsulfuron methyl representing persistent organic pollutants (POPs) was studied. Batch reactor experiments conducted with different doses of TiO_2 and a small amount of PAC of 0.05 g/L revealed that the TOC removal efficiency can be significantly increased up to 80%. Further, the concentration profile and the rate constant showed superior photocatalysis performance in the presence of PAC. The PAC added during the photo-oxidation absorbed the intermediate compounds and thereby promoted the photocatalytic oxidation. The photooxidation with a detention time of 0.5 to 2 hours resulted in intermediate products of smaller molecular weight substances. In this study, a detailed analysis with SPME/GC (solid phase micro extraction/gas chromatography) was made to study on the photo oxidation intermediates. Following 10 min of residence time in the batch reactor the MM partitioned to smaller molecular weight compounds (or substrate) which occurred at different peak times during the GC (12.10, 14.25, 17.40, 19.63 and 20.18 minutes). After 5 hours of residence time in batch reactor, same substrate was found to be degraded. The photo oxidation was faster when activated carbon was used together with TiO_2 . The substrate that occurred at the peak times of 19.96 and 18.32 minutes during the GC had nearly disappeared, while the peak at time 14.27 minutes was lower. Some anionic by - photoproducts was investigated by using ion-chromatography. Nitrate and nitrite ions were formed as by-photoproducts. The formation of NO_3^- and NO_2^- anions occurred was faster when PAC was added to the photo-oxidation. Similarly, SO_4^{2-} ions form during the photo-oxidation of MM. Where PAC is present in the reactor, the concentration of SO_4^{2-} ions peaked earlier at approximately 50 min and thereafter reduces

its (SO_4^{2-}) concentration. The reduction in concentration of SO_4^{2-} after 50 min may be due to a portion being adsorbed on the PAC-TiO₂ surface and a portion being transformed to SO₂. In this study, the increase in efficiency of MM degradation is similarly attributed to the adsorption of photo-products on the more surface available with TiO₂ coupled with the PAC and active sites available to react with the pollutants. This reduces the competitive adsorption on active sites of PAC-TiO₂ increasing efficiency of degradation of MM. However, complicated photo-oxidation and by-products occur during these processes, and it is difficult to determine the actual mechanism of photo-catalytic reaction on the PAC-TiO₂ surface and the role of active sites because sophisticated instruments are required to do this. Experiments with recirculated continuous reactor were also conducted by using TiO₂ and TiO₂-PAC. The coupling of PAC with continuous heterogeneous TiO₂ photocatalysis leads to a faster degradation of MM than the heterogeneous TiO₂ photocatalysis alone. The incorporation of a small amount of PAC of 0.05 g/L with 1.5 g/L of TiO₂ led to 78% removal even with a short residence time of 5.25 minutes.

The granular activated carbon (GAC) filter was found to be very effective as a pre-treatment for the removal of herbicide (MM). Fixed bed column experiments packed with GAC were conducted with different GAC bed heights (5, 10 and 15 cm) and different effluent velocities. The GAC photocatalytic hybrid system showed upto 90% removal with GAC bed depth of 10 and 15 cm. The 10 and 15 cm deep GAC columns showed a steady state of effluent concentration. The retention time of GAC followed by photoreaction was less than 10 minutes.

Recirculated photocatalytic batch reactor experiments conducted with the biological

treated sewage effluent showed effective DOC removal. After start up, with the recirculated flow of 60 mL/min the effluent DOC was reduced by 60% in a period of 180 min, and became relatively stable. There were no large differences between results obtained with various recirculation flow rates. About 70 to 75 % DOC removal was achieved using flow rates of 100 mL/min and 250 mL/min. However, with a recirculation flow of 250 mL/min, DOC removal decreased to 65% down from the 73% DOC removal obtained with that of 100 mL/min rate. This can be explained in terms of the characteristics of the plug flow reactor. The flow rates used in this study were large enough to keep the catalyst in suspension, and to promote good mass transfer between the reactants. When a small amount of PAC (0.05g/L) was added, a complete removal of DOC was observed after 250 and 300 min operation times. The addition of 0.05 g/L of PAC adsorbent to the recirculated continuous reactor facilitated better organic removal than titania photocatalyst alone. DOC removal was further increased to 75% within 30 min of operation.

The membrane photocatalysis hybrid system was used to separate catalyst from the effluent. The membrane flux was very low and fouling was high when TiO₂ was tried to be filtered through MF filter. To facilitate TiO₂ separation, (i) pH adjustment and (ii) flocculation of TiO₂ slurry were used. Although the use of pH adjustment achieved effective improvement to membrane operation, it was 15% less effective than applying a pre-treatment of flocculation of TiO₂ slurry. Photocatalysis and flocculation pre-treatment processes before MF/UF also resulted in high (over 90%) DOC removal, surpassing those achieved with mixed TiO₂ and PAC photocatalyst.

Acknowledgements

First, I would like to thank my greatest appreciation to my principal supervisor, Professor Saravanmuthu Vigneswaran for his patience, time, guidance, encouragement, throughout my studies. I would like to thank my co supervisors Dr Jaya Kandasamy, Associate Professor Huu- Hao Ngo, and Prof Archie Johnson for their support and guidance during my PhD course. I am also very grateful to Prof. Archie Johnson the Dean of Faculty of Engineering for taking his precious time for correction of my PhD thesis.

Warm thanks to all my great friends, Laszlo, Shon, Guo, Rong, Vinh, Javeed, and Wen. The teamwork and friendships developed with these people contributed greatly to my happiness and fun times we shared.

Many thanks also to The Office of Education Affairs Australia, and Office of Civil Service Commission Thailand for support and help during my PhD degree.

Most importantly, thank you to my wife and my parents for their love, for their encouragement and support. Especially my wife, Sirilak, you always had time to listen and discuss all problems with me. And most of all thank you for your love.

TABLE OF CONTENTS

Title page	i
Certificate	ii
Abstract	iii
Acknowledgements	viii
Table of contents	ix
Nomenclature	xiii
List of figures	xv
List of tables	xxi
CHAPTER 1- INTRODUCTION	1
1.1 Introduction	2
1.2 Research Objectives	9
CHAPTER 2- LITERATURE REVIEW	11
2.1 Introduction	12
2.2 Organic matter in water and wastewater	12
2.2.1 General	12
2.2.2 Characteristics of organic matter in water and wastewater	13
2.2.2.1 Persistent harmful compounds	18
2.3 Typical treatment processes in removing organic pollutants from water	19
2.3.1 Coagulation/ flocculation in removing organic pollutants from water	19
2.3.2 Adsorption	22
2.4 Advanced oxidation processes (AOPs)	32
2.4.1 TiO ₂ as catalyst	35
2.4.2 Parameter affecting Photocatalytic degradation	39
2.4.4 Previous studies on photocatalytic and adsorption photo catalytic hybrid systems	50
2.4.5 Membrane Photocatalytic hybrid system	53
2.8 Conclusion	57
CHAPTER 3 – EXPERIMENTAL INVESTIGATION	59

3.1 Introduction	60
3.2 Materials	60
3.2.1 Metsulfuron Methyl	60
3.2.2 Terra-humic (Biohumic)	61
3.2.3 Wastewaters and water used in the experiments and their characteristics	62
3.2.4 Photocatalytic powder	63
3.2.5 Activated Carbon	64
3.2.6 Jar Testers for conventional treatment processes	66
3.2.7 Photocatalytic reactor	67
3.3 Analytical methods	69
3.3.1 Total organic carbon measurement	69
3.3.2 Ion Chromatograph analyzer	70
3.3.4 Solid Phase Micro Extraction / Gas chromatography FID (SPME/GC)	70
3.3.5 Zetapotential measurement	73
3.3.6 Molecular Weight (MW) Distribution	76
CHAPTER 4 – PHOTO OXIDATION OF HUMIC SUBSTANCES IN WATER	78
4.1 Introduction	79
4.1.1 Natural organic matter (NOM) in water	79
4.2 Experimental units, materials and analysis	83
4.2.1 Photocatalysis batch reactor	83
4.2.2 Photocatalysis continuous reactors	84
4.2.3 Recirculated Photocatalysis continuous reactors	85
4.2.4 Analysis	86
4.3 Experimental description	87
4.3. Coagulation and Coagulation- Photocatalytic reaction	90
4.4 Effect of TiO ₂ concentration on photocatalytic reaction	92
4.5 Effect of pH on photocatalytic reaction	99
4.6 PAC, PAC as pre-treatment, and TiO ₂ coupled with low concentration of PAC on photocatalytic reaction	100
4.7 photocatalytic continuous reactor	108
4.8 Recirculated photocatalytic continuous reactor	110

4.9 Conclusion	112
CHAPTER 5 – PHOTO OXIDATION OF HERBICIDE IN WATER	114
5.1 Introduction	115
5.1.1 Herbicide in water	115
5.1.2 Langmuir – Heinshelwood model	116
5.2 Experimental units, materials and analysis	118
5.2.1 Analysis	118
5.3 Experimental description	120
5.3.1 Effect of TiO ₂ concentration on photocatalytic reaction in Batch Reactor	122
5.3.2 Molecular weight distribution of photodegraded products	125
5.4 Effect of pH on photocatalytic reaction	126
5.5 PAC adsorption and TiO ₂ coupled with low concentration of PAC on photocatalytic reaction	127
5.6 SPME /GC- FID analysis of the effect of TiO ₂ and TiO ₂ - PAC in batch photo reactor	130
5.7 Effect of inorganic analysis of TiO ₂ and TiO ₂ - PAC in batch reactor	141
5.8 Recirculated continuous photocatalytic reactor	143
5.9 Conclusion	149
CHAPTER 6 – GAC PHOTOCATALYSIS HYBRID SYSTEM	150
6.1 Introduction	151
6.1.1 Adsorption equilibria	152
6.2 Experimental units, materials and analysis	155
6.2.1 Experimental set up and description	155
6.2.2 Analysis	159
6.3 GAC adsorption results	159
6.3.1 Adsorption equilibrium	159
6.3.2 Effect of Filtration Rate in GAC column	161
6.3.3 Effect of Filter bed depth with GAC column	162
6.3.4 Fixed Bed Adsorption Mathematical Model	163
6.4 Continuous Photocatalysis System	170

6.5 GAC Photocatalysis Hybrid System	171
6.6 Conclusion	177
CHAPTER 7- MEMBRANE PHOTOCATALYTIC HYBRID SYSTEM	178
7.1 Introduction	179
7.2 Experimental units, materials and analysis	181
7.2.2 Membrane photo catalytic hybrid system	182
Analyses	184
7.3 Results and Discussions	184
7.3.1 Recirculated plug flow photocatalysis batch reactor	184
7.3.1 Recirculated continuous photocatalysis with TiO ₂	186
7.3.2 Photocatalysis in the presence of PAC adsorbent	189
7.3.3 Surface characterisation of photocatalyst suspensions	190
7.3.4 Photocatalyst separation	191
7.4. Conclusions	202
CHAPTER 8 - CONCLUSIONS AND RECOMMENDATIONS	204
8.1 Conclusions	205
8.2 Recommendations	209
Appendix A	211
Appendix A.1 Solid phase micro filtration (SPME) coupled with Gas Chromatography as an analytical technique for organic intermediates of photooxidation.	212
Appendix B	218
References	220

Nomenclature

a	: isotherm constants
b	: constant related to the binding energy of adsorption (L/mg)
BV	: bed volume
C	: concentration in bulk solution, mg/L
C_b	: desired concentration of adsorbate at breakthrough (mg/L)
C_e	: equilibrium concentration (mg/L)
C_{ef}	: effluent adsorbate concentration (mg/L)
C_{if}	: influent adsorbate concentration (mg/L)
C_o	: initial concentration (mg/L)
C_t	: final concentration (mg/L)
d	: depth of adsorbent's bed (m)
D_x	: dispersion coefficient in x direction (m^2/s)
DOC	: Dissolved organic carbon concentration (mg/L)
EBCT	: empty bed contact time
k	: apparent photodegradation rate constant (min^{-1})
K_{Ad}	: the adsorption coefficient
K_d	: linear equilibrium partitioning coefficient (L/mg)
k_f	: external film mass transfer coefficient of organic, m/s
K_F	: Freundlich constant indicative of the adsorption capacity
K_S	: the Monod half velocity coefficient
k_s	: particle phase mass transfer coefficient (1/s)
m	: amount of adsorbent (g)
M	: Weight of adsorbent (g)
n	: experimental constant indicative of the adsorption intensity
n_T	: effective porosity (dimensionless)
p_s	: solid density of the particles (mg/L)

q_t	: amount of adsorbate at any time t , (mg/g)
q_e	: amount of adsorbate at equilibrium (mg/g)
q_m	: saturated maximum adsorption capacity (mg/g)
q_s	: adsorbed phase concentration at the external surface of adsorbent particle (mg/g)
Q	: volumetric flow rate (L/min)
R	: radius of adsorbent particle, m
r	: correlation coefficient
t	: service time of column (h)
T	: temperature
u	: velocity of the fluid (m/s)
V	: throughput volume (L)
ε_b	: bed porosity
α	: dispersivity (m)
z	: bed depth, (m)

LIST OF FIGURES

Figure 2.1 Different fractions of DOC and their constituents (adapted from Thurman, 1985; Cho, 1998; Shon et al. 2006).....	16
Figure 2.2 Size range in the applied treatments in treating organic matters (Shon, 2006)	19
Figure 2.3 MW distribution of synthetic wastewater after ferric chloride (Shon et al. 2005)	21
Figure 2.4 structures of (a) Resorcinol (MW. 110) and (b) Phloroglucinol (MW. 126)	22
Figure 2.5 The possible electric charge in TiO ₂ and AC (Arana et al. 2003a)	26
Figure 2.6 Chemical and physical steps involved in the heterogeneous photocatalysis adapted from (Moulijn, Leeuwen & Santen 1993)	39
Figure 2.7 Different Types of photo reactors.....	47
Figure 2.8 Various types of membrane photocatalytic hybrid systems	57
Figure 3.1 MW size distribution of Biohumic from the Bioiberica Company	62
Figure 3.2 Schematic of jar testers used for conventional process testing in this study .	67
Figure 3.3 Spectral energy distribution of Sankyo Denki germicidal lamp.....	68
Figure 3.4 Schematic of stainless steel unit reactor unit (not scale) total volume of 70 mL	68
Figure 3.5 Multi N/C 2000 analyzer (Analytik Jena AG).....	70
Figure 3.6 Ion Chromatograph (Dionex DX-600)	71
Figure 3.7 a. Gas Chromatography FID (Varian star 3400 CX).....	72
Figure 3.7 b. SPME fibre 5% phenyl methylpolysiloxane with a film thickness of 100 μ m non-bonded	72
Figure 3.7 c. Gas chromatography with SPME 0.75-mm diameter splitless glass inlet liner	73
Figure 3.8 Zeta potential between liquid layer and particle (Malvern Instrument LTD 2003)	74
Figure 3.9 The plot of zeta potential versus pH and illustrated isoelectric point adapted from (Malvern Instrument LTD 2003).....	75
Figure 3.10 Zetapotential analyzer (Zetasizer Malvern 2000).....	75
Figure 3.11 High performance size exclusion chromatography (HPSEC) to measure MW distribution.....	77

Figure 4.1 Structure of fulvic (4.1a) (Buffle J.A.E 1977) and humic acids (4.1b) (Stevenson 1994).....	80
Figure 4.2 Schematic of the photo-catalytic batch reactor.....	83
Figure 4.3 Schematic of continuous reactor (T1: Mixing tank with no light source; Q1: influent and withdrawal rate; R: photo-catalytic reactor unit; L1, L2, L3 are UV lamps of 8 watts each).....	84
Figure 4.4 Schematic of the recirculating continuous flow photo-catalytic reactor with the catalyst. (T1: Mixing tank with no light source; Q1: influent and withdrawal rate; Q2: re-circulation flow; T2: re-circulation tank; R: photo-catalytic reactor unit; L1, L2, L3 are UV lamps of 8 watts each)	85
Figure 4.5 % DOC removal of NOM by FeCl ₃ flocculation (influent TOC = 10 mg/L).	91
Figure 4.6 FeCl ₃ flocculation as a pre treatment followed by photocatalytic reaction (2g/L TiO ₂).....	92
Figure 4.7 NOM (as %DOC) removal with different concentration of TiO ₂ without UV	94
Figure 4.8 NOM (as %DOC) removal with different concentration of TiO ₂	94
Figure 4.9 SPME GC peak at 5 min.....	96
Figure 4.10 SPME GC peak at 15 min.....	96
Figure 4.11 SPME GC peak at 40 min.....	97
Figure 4.12 SPME GC peak at 90 min.....	97
Figure 4.13 SPME GC peak at 180 min.....	98
Figure 4.14 SPME GC peak at 240 min.....	98
Figure 4.15 NOM removal with 2 g/L of TiO ₂ (as % DOC) at different initial levels of pH in batch reactor	100
Figure 4.16 NOM (as % DOC) removal at different concentrations of PAC	101
Figure 4.17 NOM (as %DOC) removal by using PAC as pre-treatment follow by batch photocatalytic reactor	102
Figure 4.18 NOM removal (as % DOC) with 0.05 g/L PAC and different concentration of TiO ₂	103
Figure 4.19 SPME/GC peaks PAC- TiO ₂ at 5 min	105
Figure 4.20 SPME/GC peaks PAC- TiO ₂ at 15 min	105
Figure 4.21 SPME/GC peaks at 40 min.....	106
Figure 4.22 SPME/GC peaks at 90 min.....	106

Figure 4.23 SPME/GC peaks at 150 min	107
Figure 4.24 SPME/GC peaks at 210 min	107
Figure 4.25 NOM removal (as % DOC) with 2 g/L of TiO ₂ by continuous reactor in various flowrates	108
Fig 4.26 NOM removal (as %DOC) with 2 g/L of TiO ₂ and 0.05 g/L of PAC by continuous reactor in various flow rates	109
Figure 4.27 NOM as (% DOC) removal in Recalculated continuous flow reactor at withdrawal rate of 20 mL/min.....	111
Figure 4.28 NOM as (%DOC) removal in Recalculated continuous flow reactor at withdrawal rate of 40 mL/min.....	112
Figure 5.1 The structure of Metsulfuron-methyl methyl 2-[[[(4-methoxy-6-methyl-1,3,5-triazin-2-akyl)amino]carbonyl]amino]sulfonyl]benzoate (MM), Molecular weight 381.36.....	116
Figure 5.1 Removal Metsulfuron methyl (MM) in the absence of UV light (TOC of the influent of MM solution = 10mg/L).....	123
Figure 5.2 Removal Metsulfuron methyl (MM) in the presence of UV light with different concentrations TiO ₂ (TOC of the influent of MM solution = 10mg/L). 123	123
Figure 5.3 Test of pseudo- first order rate constants according to Eq (5.4) for different doses of TiO ₂ concentration.	125
Figure. 5.4 Variation of MW distribution at different photooxidation time	126
Figure 5.5 MM removal with 2 g/L of TiO ₂ (as DOC) at different initial levels of pH in batch reactor	127
Figure 5.6 DOC removal of metsulfuron- methyl by adsorption with different concentration of PAC (TOC of influent MM concentration = 10 mg/L).....	128
Figure 5.7 DOC removal of metsulfuron-methyl.....	129
Figure 5.8 Test of pseudo- first order rate constants according to Eq (5.4) for different doses of TiO ₂ concentration.	130
Figure 5.9 SPME GC peak of metsulfuron methyl at 5 min with TiO ₂ 2g/L	132
Figure 5.10 SPME GC peak of metsulfuron methyl at 10 min with TiO ₂ 2g/L	132
Figure 5.11 SPME GC peak of metsulfuron methyl at 30 min with TiO ₂ 2g/L	133
Figure 5.12 SPME GC peak of metsulfuron methyl at 1 hour with TiO ₂ 2g/L	133
Figure 5.13 SPME GC peak of metsulfuron methyl at 2 hour with TiO ₂ 2g/L	134
Figure 5.14 SPME GC peak of metsulfuron methyl at 3 hour with TiO ₂ 2g/L	134
Figure 5.15 SPME GC peak of metsulfuron methyl at 5 hour with TiO ₂ 2g/L	135

Figure 5.16 SPME GC peak of metsulfuron methyl at 7 hour with TiO ₂ 2g/L	135
Figure 5.17 SPME GC peak of metsulfuron methyl at 5 minutes with TiO ₂ 2g/L and 0.05 g/L PAC	136
Figure 5.18 SPME GC peak of metsulfuron methyl at 10 minutes with TiO ₂ 2g/L and 0.05 g/L PAC	137
Figure 5.19 SPME GC peak of metsulfuron methyl at 30 minutes with TiO ₂ 2g/L and 0.05 g/L PAC	137
Figure 5.20 SPME GC peak of metsulfuron methyl at 1 hour with TiO ₂ 2g/L and 0.05 g/L PAC	138
Figure 5.21 SPME GC peak of metsulfuron methyl at 2 hour with TiO ₂ 2g/L and 0.05 g/L PAC	138
Figure 5.22 SPME GC peak of metsulfuron methyl at 3 hour with TiO ₂ 2g/L and 0.05 g/L PAC	139
Figure 5.23 SPME GC peak of metsulfuron methyl at 5 hour with TiO ₂ 2g/L and 0.05 g/L PAC	139
Figure 5.24 SPME GC peak of metsulfuron methyl at 7 hour with TiO ₂ 2g/L and 0.05 g/L PAC	140
Figure 5.25 Formation of (a) nitrate and (b) nitrite during the batch photocatalysis batch system (2g/L of TiO ₂ alone (solid line) and 2 g/L TiO ₂ with 0.05 g/L of PAC (dotted line)).....	141
Figure 5.26 Formation of sulfate anion by using TiO ₂ 1 g/L (solid line) and 1 g/L TiO ₂ with PAC 0.05 g/L (dotted line).....	142
Figure 5.27 (a-c) DOC removal by recirculated continuous photo-catalytic reactor....	145
Figure 5.28 a-b. Test of pseudo- first order rate constants according to Equation (9) at different withdrawal rate and (a) with TiO ₂ alone and (b) TiO ₂ and 0.05 g/L PAC.	147
Figure 6.1 Comparison between Langmuir and Freundlich isotherm (Cooney, 1999)	154
Figure 6.2 Schematic of GAC adsorption system.....	157
Figure 6.3 Schematic of GAC photocatalysis hybrid system	158
Figure 6.4 Adsorption equilibrium of metsulfuron methyl by GAC with different isotherm models (contact time = 72 hours, mixing rate 130 rpm, temperature 25°C)	160
Figure 6.5 Influence of filtration rate on the performance of adsorption of a 5 cm deep GAC bed. Average influent TOC= 10mg /L.....	161

Figure 6.6 Variation of TOC removal efficiency of GAC adsorption for different GAC bed depth. Filtration rate is 4m/h	163
Figure 6.7 Variation of C/C_0 of the GAC filter for various filter bed depths.	167
Also shown is the fit between experimental data and model simulation for variation in bed depth. Filtration rate = 4 m/hr, average influent TOC = 10 mg/L. $k_f = 1.2e^{-5}$ and $k_s = 4e^{-8}$ for all modelling runs.	167
Figure 6.8 Variation of C/C_0 of the GAC filter for various filtration rates. Also shown is the fit between experimental data and model simulation for variation in bed depth. Bed depth = 5 cm, average influent TOC = 10 mg/L.....	168
Figure 6.9 DOC removal by continuous photo catalytic reactor at various flow rates of 4, 10, 20 and 40 ml/min	171
Figure 6.10 Comparison of DOC removal of MM herbicide with flow rate 4 ml/ min and 10 mL/min with 5 cm deep bed of GAC.....	175
Figure 6.11 Comparison of DOC removal of MM herbicide with flow rate (A) 20 ml/ min and (B) 40 mL/min with 5 cm deep bed of GAC.....	175
Figure 6.12 Comparison of DOC removal of MM herbicide after 10 cm deep bed of GAC.	176
Figure 6.13 Comparison of DOC removal of MM herbicide after 15 cm deep bed of GAC.	176
Figure 7.1 Schematic of photocatalytic batch reactor system.....	182
Figure 7.2 Schematic of the MF/UF experimental unit	183
Figure 7.3 DOC removal of synthetic wastewater with various flow rates (conditions $TiO_2 = 1.5$ g/L, $Q_1 = 60, 100, 250$ mL/min, R ; L1, L2,L3 = 8 Watts UV Lamps each)	185
Figure 7.4 DOC removal of synthetic wastewater with various flow rates (conditions; $TiO_2 = 1.5$ g/L, and PAC 0.05 g/L $Q_1 = 60, 100, 250$ mL/min, L1, L2, L3 = 8 Watts UV Lamps)	185
Figure 7.5 Photocatalytic DOC removal with 1.5 g/L TiO_2 catalyst (Figure 4.4 ($Q_1 = 10, 20, 40$ mL/min, $Q_2 150$ mL/min R: photo-catalytic reactor unit; L1, L2, L3 are UV lamps of 8 watts each).....	187
Figure 7.6 Photocatalytic DOC removal with 1.5 g/L TiO_2 and 0.05 g/L PAC (Figure 4.4 ($Q_1 = 10, 20, 30, 40$ mL/min, $Q_2 150$ mL/min R: photo-catalytic reactor unit; L1, L2, L3 are UV lamps of 8 watts each).....	189

Figure 7.7 Variation of zeta potential (ZP) with a treated suspension (1.5 g/L of TiO ₂)	190
Figure 7.8 Screen showed stepwise method increase of flux, 10 to 15 min monitoring of the TMP trendline (start at 2.09.32 pm. end at 2.25 45 pm.).....	194
Figure 7.9 second screen showed stepwise method increase of flux, 10 to 15 min monitoring of the TMP trendline (start at 2.09.46 pm. end at 2.30.02 pm.).....	194
Figure 7.10 Third screen showed stepwise method increase of flux, 10 to 15 min monitoring of the TMP trendline (start at 2.28.07 pm. end at 2.40.30 pm.).....	195
Figure 7.11 Fourth screen showed stable TMP trend, and this value was reported as the critical flux	195
Figure 7.12 Settled turbidity versus coagulant dosage (wastewater slurry with 1.5 g/L of TiO ₂ (Feed 40 mL/min; Feed 2 10mL/min).....	198
Figure 7.13 Effect of coagulant dosage on ZP and pH feed 1	199
Figure 7.14 %DOC removal with different coagulant dosage with raw synthetic waste water	199
Figure7.15. Critical fluxes 1: raw wastewater, 2: Feed 1 pH adjusted, 3: Feed 2 pH adjusted, 4: Feed 1 flocculated, 5: Feed 2 flocculated, 6: Feed 3 (photocatalyst together with PAC)	201

LIST OF TABLES

Table 2.1 Removal of EDC and PPCP from BTSE by PAC adsorption (adapted from Snyder et al., 2006; Westerhoff et al., 2005, Shon et al., 2006)	25
Table 2.2 Removal of EDC and PPCP with full scale GAC biofilter (ng/L) (Snyder et al., 2006; Shon et al., 2006)	28
Table 2.3 Typical biofilter design parameters used in tertiary wastewater and surface water treatment (adapted from Rachwal et al., 1996)	31
Table 2.4 List of the DOC removal by filtration with biological treated sewage effluent (BTSE)	31
Table 2.5 Advanced oxidation processes used in water treatment (Shon et al., 2006) ..	33
Table 2.6 Bandgap energies from some common semiconductor materials at 0 K (Adapted from Serpone and Pelizzetti 1989 and Schiavello and Sclafani 1997, Sakthivel et al. 2000, Thiruvengkatachari et al. 2007)	37
Table 2.7 Overview of various reactor types	48
Table 2.8 Review of organic pollutants removal by AOPs hybrid system adapted from Shon et al., 2006.....	50
Table 2.9 Easily oxidized organic compounds by photocatalytic processes (adapted from Pirkanniemi and Sillanpää, 2002; Shon et al., 2006)	52
Table 3.1 Specification of Metsulfuron methyl	61
Table 3.2 Constituents of synthetic wastewater that used in experiments.....	63
Table 3.3 Characteristics of the TiO ₂ P25 Degussa photocatalytic powder used in the present experiments.....	64
Table 3.4 Characteristics of Powdered Activated Carbon (PAC) used (James Cumming & Sons Pty Ltd., Australia).....	65
Table 3.5 Physical properties of granular activated carbon GAC (Calgon Carbon Corp., USA)	66
Table 3.6 Sankyo Denki UV lamp specification.....	67
Table 4.1 pH and photocatalysis	99
Table 5.1 Variation of rate constant at different concentrations of TiO ₂	125
Table 5.2 Apparent rate constants obtained at different concentrations of TiO ₂ and at PAC concentration of 0.05 g/L	129

Table 5.3 DOC removal at different detention time (MM concentration =10 mg/L, TiO ₂ = 1.5 g/L, PAC = 0.05 g/L).....	143
Table 5.4 Variation of pseudo first order rate constant obtained from Equation (9) at different withdrawal rates of 1.5 g/L TiO ₂	148
Table 5.5 Variation of pseudo first order rate constant obtained from Equation (9) at different withdrawal rate of 1.5 g/L TiO ₂ and 0.05 g/L PAC	148
Table 6.1 Equilibrium adsorption isotherm parameters.....	159
Table 6.2 Parameters used for model simulation of GAC filter	166
Table 6.3 DOC removal at different retention time (MM concentration = 10 mg/L, TiO ₂ =1.5 g/L , reactor volume 210 mL, 8 W UV light three lamps)	171
Table 6.4 DOC removal at different retention time (MM concentration =10 mg/L, TiO ₂ = 1.5 g/L, PAC = 0.05 g/L , reactor volume 210 mL, 8 watts UV light, 3 lamps and after GAC adsorption at bed depths of 5, 10, and 15 cm.	173
Table 7. 1. Characteristics of raw wastewater and TiO ₂ treated suspensions.....	191
Table 7.2. Jar test results with 1 g/L of TiO ₂ treated suspensions	197
Table A.1 Limits of detection for 50 minute extraction of selected herbicides adapted from (Boyd-Boland & Pawliszyn 1995)	213
Table A. 2 Relative factor of increase of K at humic acid concentration (C _H , in mg/L) of 0,20,100,500 mg/L; expected relative factor of increase based on the mass balance (C _{calc}) and the logarithm of the octanol – water partitioning coefficient (log K _{ow}) applied in the mass balance (Dewulf, Van Langenhove & Evaraert 1997)..	215
Table A.3 Application of SPME/ GC to the identification of herbicides in aqueous sample (LOD; limit of detection, DI ; direct insertion, HS; head space, PDMS; polydimethylsiloxane, PA; polyacrylate, DVB; Divinylbenzene, CAR; Carboxen, CW; Carbowax, TPR; Templated resin)	217